Check for updates

Photoreversible Loading and Unloading of Q–Silsesquioxane Dynamic Network Sponges

Nai–hsuan Hu and Joseph Coy Furgal*

The synthesis and mechanical properties of photoswitchable silsesquioxane/azobenzene hybrid 3D-polymers ("dynamic sponges") are presented and discussed. The hybrid is capable of extensive macroscopic movement, and overcomes previously problematic crosslink locking issues. A hydride-functionalized Q-type silsesquioxane ($Q_8M_8^H$) is reacted with di-allyloxyazobenzene using hydrosilylation methods. The properties of the resulting materials are controlled via careful choice of starting material ratios and solvent, leading to gels or films. Both morphologies show pronounced photoresponsive behavior in and on the surfaces of different solvents. Photoactuation is tracked by microscopy, dynamic mechanic analysis, and UV–vis spectroscopy. The gel system has a porous structure similar to a sponge. It undergoes shrinkage in volume by 18.3% in toluene under UV irradiation, and shows excellent recovery to the swollen state after irradiation with visible light. These novel photodynamic materials offer reversible modulus switching from 160 kPa in the swollen state to 500 kPa in the "wrung-out" sponge. The sponges can engage in uptake and release of a range of substances (i.e., reversible hydrophobic sponging), with overall performance determined by solvent specific quantities such as polarity and size. Such behavior gives these materials high potential for soft robotics applications and great promise as reusable environmental remediators.

1. Introduction

Stimuli-responsive polymers are part of the exciting and rapidly expanding field of smart materials. This area of research has seen many significant breakthroughs in the past decade.[1,2] Smart micro/nanoparticles,[3,4] surface-tethered materials,[5,6] and shape memory polymers[7,8] are just a few recently reported examples of such highly functional, novel structures. Light-stimulated materials (i.e., photoresponsive polymers) have received much attention because they can be manipulated both spatially and temporally using specific wavelengths of light.[9,10] To achieve precise control of polymer properties, a photo-responsive moiety is typically incorporated into a macromolecular system to function as a trigger. The structure and/or functionality of the trigger affect the overall characteristics of the polymer, giving the system the ability to switch properties with light. This "on-demand" feature has been developed for drug delivery,[11] ion/gas sensing,[12–14] self-assembly,[15,16] and mechanically actuating systems.[17–19]

A large number of photoresponsive units that can undergo reversible transformation between two molecular structures have recently been reported.[20–22] Because of their conversion efficiencies and compatibility with other systems, diarylethene, spiropyran, and azobenzene structures are the most commonly studied photoactuators. In particular, the main characteristics of the azobenzene unit have been elucidated in detail.[23–26] Through cis-trans isomerization, the dipole moment of azobenzene changes from 0.5 to 3.1 D and its molecular length switches between 9.9 and 5.5 Å.[27,28] These features make it feasible to create materials for photo-patterning or photo-mechanical actuation.[29,30] Isomerization of azobenzene does not require electron transfer, this means that the switching process has less chance of being interrupted by other molecules or ions in the system. Preserving photo-switch functionality makes azobenzene-based systems attractive for use in a wide range of polymer systems.
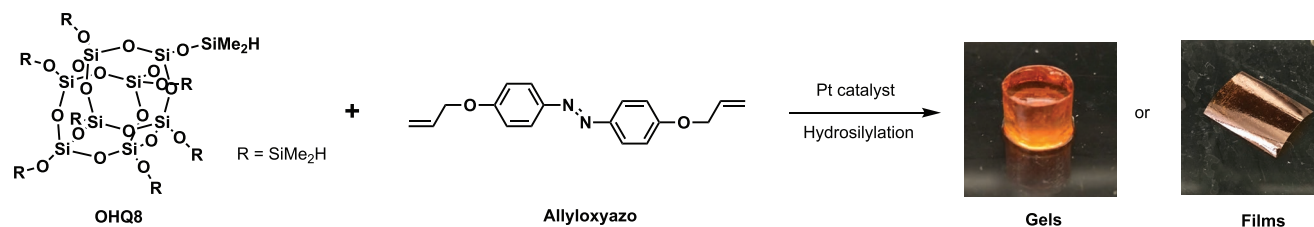
Many attempts have been made to incorporate azobenzene into polymers as a photo-responsive trigger. Typically, this leads to changes in the absorption wavelength, morphology, and rheology upon irradiation.[31–37] Researchers have also focused on the possibility of using azobenzene to convert molecular movement into the macro scale. Success has been achieved in terms of triggering reversible curvature in materials,[38–44] with the major focus on liquid crystalline (LC) monomers and polymers,[45–48] but few outside of hydrogels have delivered actuation as a true photodynamic sponge.

Sponge materials have high porosity and are able to soak up large amounts of solvent and dissolved substances.[49,50] By making sponges photodynamic, these materials can potentially both soak up large amounts of a substance and subsequently, by irradiation with an alternate wavelength of light or via thermal relaxation, expel their cargo and return to their native state. Such reversibility requires implanting functional groups that can alter the porosity of the sponge system by changing

N.–h. Hu, Prof. J. C. Furgal
Department of Chemistry
Center for Photochemical Sciences
Bowling Green State University
Bowling Green, OH 43403, USA
E-mail: furgalj@bgsu.edu

The ORCID identification number(s) for the author(s) of this article can be found under https://doi.org/10.1002/adfm.202010114.

**ADVANCED
SCIENCE NEWS**
www.advancedsciencenews.com

**ADVANCED
FUNCTIONAL
MATERIALS**
www.afm-journal.de

Scheme 1. Reaction for synthesis of $Q_8M_8^H$/allyloxy-azo gel or film.

the pore shape and/or its polarity. An example is a host–guest cross-linking supramolecular hydrogel consisting of azobenzene and cyclodextrin, developed for biological applications such as drug or gene delivery.[51–53] The geometry changes force the guest azobenzene to leave the host, leading to an expansion in host size. Takashima et al. successfully prepared a reversible photo-actuated hydrogel that can expand to 124% of its original volume and then contract back to 104%.[54] This result shows the potential of azobenzene gels for artificial muscles, light-triggered motors, or reusable environmental remediators.

However, there are some disadvantages to the system described above. First, hydrogel systems are limited to aqueous solutions and the range of molecules that the dynamic sponge can absorb is restricted by their polarity.[55] Second, host–guest interactions can easily be affected by molecules with a molecular size and shape similar to azobenzene, since they may also be able to fit in the host and hinder the actuation mechanism. Although host–guest hydrogel systems are a breakthrough in this field of research, an alternative actuation method or material backbone is needed if these materials are to be used in environmental remediation or artificial muscle systems. In this paper, we present a new methodology based on fully covalently bonded systems in silicon-based materials to overcome these limitations, improve stability, and broaden their potential applications.

Over the past few decades, silicon chemists have shown great interest in the preparation of responsive siloxane gel systems; most notably using liquid crystal or polymeric elastomers.[56–61] The most famous example of this was achieved by Finkelmann et al. which used a methylsiloxane polymer functionalized with mesogens that could be mechanically aligned in a two-step synthetic process.[62] Guo et al. have also developed a polysiloxane with side chain azobenzene mesogens that crystallize into lamellar structures during self-assembly resulting photoresponsive phase change behaviors.[58] Using the photoisomerization of azobenzene, the mechanical properties of the polymer can be altered by light-driven structural rearrangements. In some cases, this internal photoisomerization is large enough to overcome polymeric rigidity and render observable macroscopic mechanical motion.[59,60] However, instead of directly using the change of dipole and length changes of the molecule, most of these cases use phase transition as driving force to obtain a more global shape change. These materials tend to have low levels of true cross-linking and the resulting products tend to be structurally fragile. Furthermore, synthetic methods in LC materials tend to be quite involved and rely on very specific conditions to get molecular alignment by force or self-assembly.[48]

To use the isomerization force of azobenzenes more directly, a less complex structure with low rigidity is needed. With silsesquioxane networks based on silicon-oxygen cages, which have better structural order and are much stiffer, visible contraction/expansion behavior through a hybridization effect of hydrogel and LC systems can be achieved. Guo et al. tried to incorporate azobenzene into polyhedral oligomeric silsesquioxanes (POSS) systems.[61] Their results showed cis-trans isomerization in UV–vis spectra, but offered little to no changes in macroscopic shape. Abboud et al. have also attempted to imbue macroscopic shape changes on in situ formed silsesquioxane networks with azobenzene linkers, also without visible actuation being achieved.[63] Our materials overcome these limitations by carefully adjusting the cross-linker ratios and installing a slightly more flexible POSS cage that reduces the total rigidity of the material allowing for slight network rearrangement and dynamic shape changes in both films and bulk network gels.

Our photoactuatable POSS/azobenzene silicon-hybrid polymer system consists of 4,4′-di-allyloxyazobenzene (allyloxy-azo) coupled to octakis(dimethylsiloxy)silsesquioxanes ($Q_8M_8^H$, Q-type POSS) cages (**Scheme 1**) using Karstedt's catalyst in either toluene or dichloromethane (DCM). This methodology was developed out of previous research on $Q_8M_8^H$ network polymers that showed considerable reversible swelling characteristics and amorphous periodicity suggesting long range order in structure.[64] These Q-type POSS cages have a rigid inner core and a single dimethylsilane unit at each corner, offering a short flexible buffer between the cage and the azobenzene unit, increasing reaction intermediate solubility and arrangement potential for effective synthesis, and also giving the material better photoresponsive behavior by increasing the elastic properties of the materials. Photoresponse is achieved by imbuing both shape and phase change potential by combining properties of LC elastomers and hydrogels,[48,65] with the conceivability of a loosely correlated nematic-to-isotropic shape change.[43,45] Additionally, these cages are environmentally friendly since they can be derived from agricultural waste such as rice hull ash.[66,67] Note that there was no specific design intent to embed molecular order in these systems using the bulk synthetic methods described herein and any network ordering is achieved by coincidence. The overall simplicity of the synthetic method makes it highly attractive for large scale synthesis, since little processing to adjust network structure is undertaken beyond initial synthesis.

We began our investigation looking at films of the network materials, due to the ease of synthesis and believed higher propensity for fast and efficient photoresponse due to better light penetration.[60] We then expanded our work to a primary
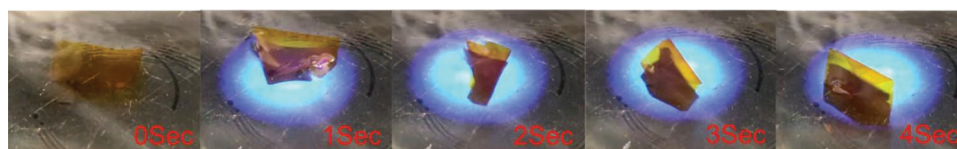
**ADVANCED
SCIENCE NEWS**

www.advancedsciencenews.com

**ADVANCED
FUNCTIONAL
MATERIALS**

www.afm-journal.de

Figure 1. Actuation of 1:2 (POSS:Azo) ratio film under 365 nm UV irradiation.

focus in the development of gel-based systems since they have more favorable mechanical and physical properties for use in environmental remediation and soft robotics (i.e., to act as reversible sponges in the solvent swollen state, which is different than the solid state performance sought after with LC's). To the best of our knowledge, the results described below represent the first successful attempt to create a silsesquioxane-based network organogel with the ability to show reversible macro scale expansion and contraction, and to expel and soak up fluids under photoirradiation.

2. Results and Discussion

Photoresponsive $Q_8M_8^H$/di-allyloxyazobenzene (POSS/Azo) polymer were synthesized as described in the Experimental Section by hydrosilylation reaction in either toluene or DCM at ratios described below in the text. The materials were designed to photoactuate in the swollen or solvent bedded state based on knowledge of swelling characteristics of previous POSS network studies.[64,68] These materials were characterized by Fourier-transform infrared spectroscopy (FTIR), thermogravimetric analysis (TGA), scanning electron microscopy (SEM), dynamic mechanical analysis (DMA), rheometry, Brunauer–Emmett–Teller (BET) surface area analysis and UV–vis spectroscopy, with spectra shown in the text, the Supporting Information, and with further synthesis details given in the Experimental Section.

2.1. Cross-Linker–4,4′-Di-allyloxyazobenzene Photophysics

The allyloxy-azo di-functional cross-linker used in this paper has been used in previously published investigations,[61] however an examination of the monomers base photophysical properties has not been well established on their own. UV–vis spectroscopy was used to better quantify actuation efficiency, and the quantum yield of the isomerization of the cross-linker. For trans form, the π–π^* transition can be found at 358 nm (Figure S1a, Supporting Information). Under UV (365 nm) irradiation (17 mW cm^{-2}), a decline in the π–π^* transition was observed, which implies reduction of trans form azobenzenes. The growth of cis form π–π^* transition at 309 nm also verifies isomerization behavior. Additionally, absorption of n–π^* forbidden transition for both cis and trans forms overlap at 450 nm. The reverse isomerization happens with irradiation (15 mW cm^{-2}) of 505 nm visible light. The wavelength was chosen to avoid overlap between π–π^* and n–π^* absorptions. The quantum yield of photoisomerization from trans to cis form was calculated to be 0.73 ± 0.01 by the Stranius and Börjesson method,[69] with trans form as the photostationary state, and showing remarkable efficiency for an azobenzene

moiety (see Supporting Information for QY calculation data).[25] This high quantum yield led us to believe that this cross-linker would perform admirably after being incorporated into materials.

2.2. Photoresponsive Films

Development of responsive materials began with the synthesis of thin films. For materials with similar structure, a thinner form has a higher chance to perform actuation by reducing light penetration issues.[60] Since over-crosslinking and low flexibility has been a factor in diminishing photoactuation for silsesquioxane networks,[59,60] a 1:2 (POSS:Azo) molar ratio was chosen as our starting point to render reasonable crosslinking without over locking the system, which would prevent photoresponse. All ratios used are based on molecular stoichiometry (1 mol POSS to 1 mol azobenzene, 1:1). This results in the likelihood of imbuing some molecular order into the material to add slight phase change propensity to the molecular length, and polarity changes, expected in the material upon photoactuation. Films with a thickness of 0.03 mm were synthesized on the surface of a glass slide in toluene with a 1:2 (POSS:Azo) ratio using the reaction shown in Scheme 1. Azobenzene incorporation and the extent of Si−H groups reacted by hydrosilylation was verified by FTIR and TGA, and is shown in Figure S2, Supporting Information.

The films were tested for their photoactuation behavior and mechanical properties. Irradiation of the film on the surface of toluene with a 25 mW cm^{-2} 365 nm LED leads to rapid folding or flipping (**Figure 1**). This is caused by tension building up in the film due to isomerization and subsequent shortening of the azobenzenes on the irradiated side of the sample. Once the film rolls, the side originally on the bottom is exposed to light, causing reverse rolling[70] This process repeats ≈6 times until azobenzene on both sides reaches their maximum ratio of cis isomers and stays flat (see Video S1, Supporting Information). Film mechanical properties are discussed below in Section 2.6, where they are compared and contrasted with gels. The surprisingly agile photoresponsive behavior of the films led us to explore methods to expand to thicker and more robust materials with higher application potential.

2.3. Photoresponsive Gels

Photoresponsive gels were synthesized in DCM instead of toluene since it gave much better dissolution of $Q_8M_8^H$ and also offered much faster gelation. These were conducted in the same 1:2 (POSS:Azo) ratio used for the films. The density of the resulting gels was lower than DCM, causing them to float
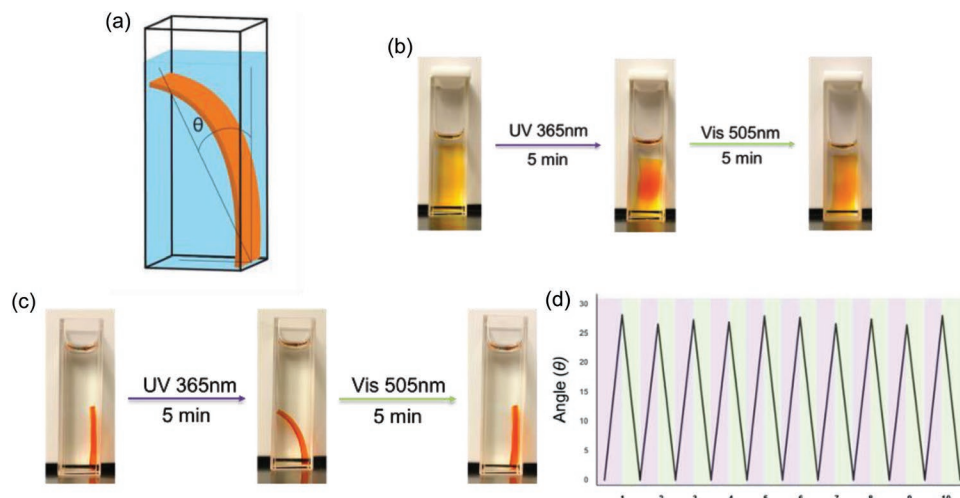
Figure 2. a) Angle measurement method for gels. b) Front and c) side of a 1:2 (POSS:Azo) gel irradiated with UV 365 nm and vis 505 nm light. d) Repeat experiments of actuation for the gel over 10 cycles.

in solution. Due to surface exposure, the tops of the gels dried out, making them difficult to analyze. Therefore, gels from the reaction in DCM were solvent exchanged with toluene for further study where they could be completely covered in solvent. The solvent change from DCM to toluene affects the overall volume of the gel (smaller in toluene), a more compact structure might limit actuation of the gels. However, this process is necessary for analysis and did not appear to affect the overall network structure significantly.

The resulting gel was cut into rectangles to observe actuation behaviors in a toluene bath (**Figure 2**a). In a cuvette, the irradiated area turns reddish orange with 17 mW cm^{-2} of 365 nm UV light, and turned back to mild orange with 27 mW cm^{-2} of 505 nm green light (Figure 2b). After irradiation, the majority of structural shift to the cis form of azobenzene increases the possibility of π–π stacking and a higher internal dipole moment, resulting in a red shift in color. By UV–vis, besides the existing π–π^* transitions, a broad shoulder appears at 425–525 nm (Figure S2b, Supporting Information). This broad peak likely results from the accumulation of π–π overlapping within the

system and indicates energy transfer between azobenzenes in the polymer; this also contributes to the photochromism leading to the appearance of red colors. An unusual weak absorption is also observed at 775 nm, which likely stems from the absorption of red light by the material upon photochromism.

Besides a clear color change, minor shrinkage at the irradiated area was also observed. Since the side of the gel facing UV light receives higher intensities, 28 degrees of curving was observed as a result of uneven contraction. (Figure 2c). The repeatability of these behaviors is confirmed over 10 cycles of actuation without loss of responsive behavior (Figure 2d). This led us to hypothesize that our POSS/Azo system can function as a photodynamic system, changing size by photoinduced isomerization (**Figure 3**a). To test the actuation ability of the gel, a 1:2 (POSS:Azo) gel was cut to 4.5 mm × 4.5 mm with 1.3 mm thickness. It was then irradiated with 14 mW cm^{-2} of 365 nm UV and 1.7 mW cm^{-2} of 560 nm visible light in a toluene bath and imaged under a microscope (Figure 3b). An 18.3% volume change (shrinkage) was recorded, and reversible cycling over three iterations was observed (Figure 3c).
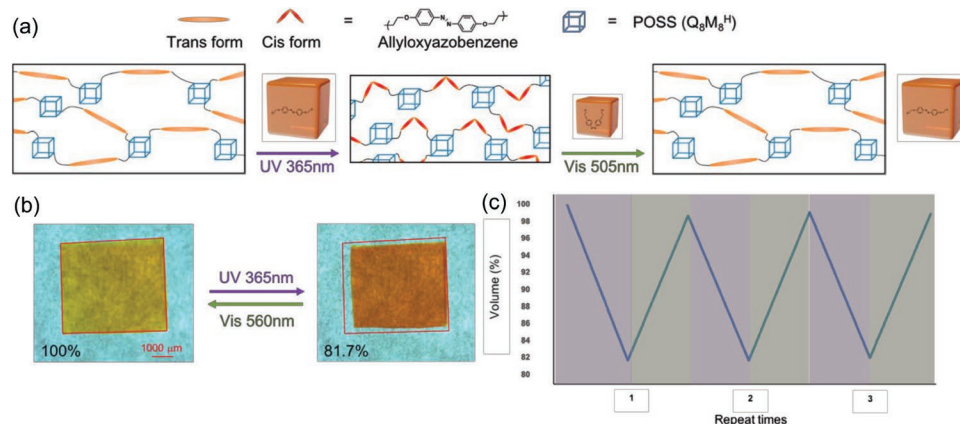

Figure 3. a) Illustration for actuation of the POSS/Azo hybrid gels. b) Contraction and expansion for the 1:2 (POSS:Azo) ratio gel. c) Actuation repeatability test for the gel over 3-cycles.
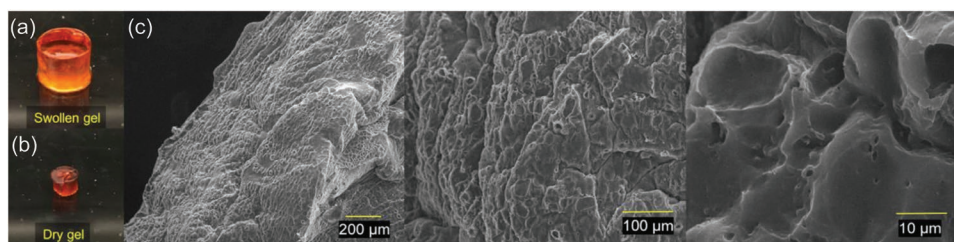
Figure 4. a) Swollen and b) dried forms of 1:2 (POSS:Azo) gel removed from reaction vial and c) SEM images from dried gel.

The photoresponsive behaviors of the 1:2 (POSS:Azo) led us to further investigate the structural properties of the gel to try and determine what influence porosity had on the swelling behavior. We anticipated that the gel would have reasonably high surface area and porosity in the micro/meso region in the dry state. This is based on similar network POSS materials having intrinsic porosity.[71] Porosity was measured after the gel was air and vacuum dried using a BET method. The volume of the dried gel was 23.5% of DCM swollen gel before being ground for analysis. Surprisingly, in our analysis of BET surface area, neither mesopore nor micropore range volumes were found in these systems and the material had effectively no intrinsic surface area.

This led us to further investigate the material itself by SEM analysis. By SEM, pore structure with large diameters of ≈15 to 20 µm was observed (**Figure 4**). With pores of this size BET analysis is usually a poor indicator of surface area. Another caveat is the swellability of the material itself. Even if the pores are one size in the solid state, they will expand to a maximum volume when loaded with solvent. Knowing that the volume of swollen gels is about four times larger than dried gels, the size of the pores in swollen gel can be estimated at ≈60 to 80 µm after expansion.

2.4. Formulations and Solvents

The fulfillment of strong contraction and expansion of the materials above with 1:2 (POSS:Azo) molar ratio and showing their expandable porosity led us to explore materials with other ratios, and quantify their photoresponse (**Figure 5**a). POSS and Azo were mixed in 1:1 to 1:8 ratios to determine which ratio maximized the volume and modulus changes caused by photoisomerization (Table S1, Supporting Information). The cross-link density was also further adjusted by partially replacing the 3D starting material $Q_8M_8^H$ POSS (8 reactive positions) with linear polydimethylsiloxane (PDMS, 2 reactive positions, MW450 and MW4500) to see if softening the material gave more favorable contraction/expansion events and make it more similar in structure to LC type elastomers. For example, a sample with 25% PDMS means 25% molar ratio of POSS were substituted with the same mols of hydride terminated PDMS reducing cross-link density. The reaction solvent volume was also varied to determine the effect of concentration on the density of formed gels (Figure 5a). The reaction completion for POSS can be interpreted by the peak of H-Si(Me)$_2$ resonance in IR spectra at 2150 cm^{-1} (Figure S5, Supporting Information) and the ceramic yields (CY) obtained from TGA analysis (Figure S3a and Table S1, Supporting Information), where TGA burnout in air corresponds to the amount of silica remaining after organics are removed. Results from 1:4 and 1:8 ratios show little remaining reactive corner for POSS, implying high reaction completion. Remaining Si—H groups can be useful in future post-synthesis modifications. TGA analysis (air) also shows expected values for CY suggesting Azo incorporation as anticipated. Note that the values of theoretical CY are lower than found CY due to the incomplete burnout of dimethylsilyl groups.[71] Ratios of 1:2 and 1:4 showed gelation within 24 h, which was expected based on their selected ratios to develop networks. Products from 1:1 and 1:8 ratios stayed soluble in DCM, with 1:1 resulting in
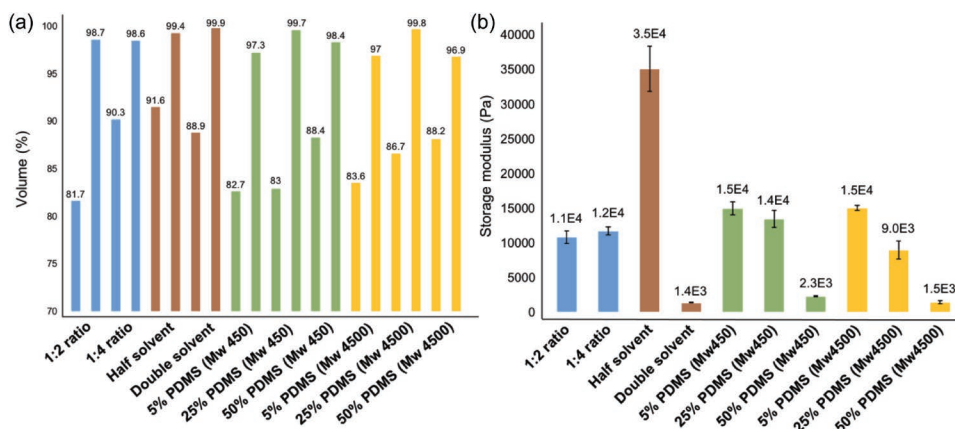

Figure 5. a) Volume change from 100% upon UV irradiation (left bar), and return to swollen state upon switching to visible light (right bar) for each of the toluene solvent exchanged gel materials. b) Storage modulus for toluene swollen gels with different compositions.

**ADVANCED
SCIENCE NEWS**
www.advancedsciencenews.com

**ADVANCED
FUNCTIONAL
MATERIALS**
www.afm-journal.de

semi-linear polymers, and 1:8 as Azo functionalized full cages, showing little linking. This would be more similar in structure to a fully decorated POSS cage.[72] Due to the lack of gelation, 1:1 and 1:8 ratios were not explored further. Gels of 1:2 and 1:4 show excellent response to UV and vis light, and can be swollen back to at least 96.9% of their original volumes after dry out. The gel with 1:4 ratio shows a slightly lowered ability of contraction than 1:2 due to a higher degree of cross-linking. This higher cross-linking is confirmed by TGA, which shows a greater percentage of cross-linker leading to lower CY. The amount of solvent used for synthesis (1:2) seems to have little influence on the degree of cross-linking established within the gel (Figure S3b, Supporting Information). The IR spectra show few differences between these two experiments (Figure S6, Supporting Information). However, reactions with less solvent result in higher densities (i.e., less swelling) due to more spatially confined reactions between cages, which in turn lowers the contraction abilities of the gels. The double solvent systems in theory should result in higher swelling abilities due to their more spaced out POSS cores, which is evident in the rheological data of Figure 5b. While the overall swelling potential of all the 1:2 (POSS:Azo) ratio systems is similar upon solvent exchange, the original concentration still performs the best, suggesting that this is an optimal preparation in terms of the balance between network structure building effects and contraction abilities.

Samples with PDMS substitutions similarly show less contraction with higher replacement ratios. This was unexpected, but is because the flexible long chain structure of PDMS in the gel counteracts the force caused by azobenzene isomerization. Gels with short chain PDMS (MW450) substitution generally perform better actuation than those with long chain PDMS (MW4500) due to elastic energy absorption.[73] TGA experiments verify the structural changes by showing lower CY with higher substitution ratios (Figure S3c,d, Supporting Information). This indicates that POSS's are less cross-linked with higher percentage of substitution.

Rheological experiments were also conducted to determine relative material stiffness in their toluene swollen state. The storage modulus data are compared as an indicator of flexibility of the gel and their ability to retain or restore shape (Figure 5b). 1:2 and 1:4 (POSS:Azo) ratio gels show similar results of ≈12 kPa. As expected, gels from reactions with half solvent are much less flexible than those with double solvent due to increasing lubricity and swelling potential with a more spaced out gel structure, from the lower concentration reaction.

This allowed for more space within the network for solvent to come in, but did not greatly influence actuation potential. The structure would now allow for the solvent to move within it, whereas a denser gel (half solvent) is too stiff to result in good actuation. Gels with 5% PDMS are generally slightly less flexible than samples with only $Q_8M_8^H$. With higher percentage of PDMS substitution, chain structure fills in the spaces between POSS, buffers movement and gives the gels greater flexibility, although at the expense of porosity. Overall, samples with our initial 1:2 (POSS:Azo) ratio showed the best performance among all samples with 18.3% of contraction and only 1.3% of volume lost after re-expansion in toluene. This specific ratio was therefore applied to additional actuation experiments.

Volume changes were explored in various solvent systems to determine overall compatibility (**Figure 6**a). Samples synthesized from DCM were cut to 4.5 mm × 4.5 mm with 1.3 mm thickness and then soaked in 20 mL of different solvents overnight to finish solvent exchange. For reference the dry 1:2 (POSS:Azo) gel shrinks to 23.5% of DCM swollen volume. Methanol, ethanol, isopropanol, and 5w-30 motor oil were tested; however, these solvents are not compatible with the gel system. Studies with these samples show DCM diffusing into the exchange solvents while the gels themselves shrink.

For compatible solvents, the volume of the gel seems to be determined by a complex combination of size, polarity, and structure of the solvent molecule, which can be described as overall solvent quality for the system. However, generalizations can be dangerous, and here we simply discuss the overall trends. Figure 6a shows the overall swelling of materials versus a 100% swelling standard with DCM. Tetrahydrofuran (THF) through m-xylene all show good swelling above 90%, which then corresponds to high actuation efficiency as shown in Figure 6b. The latter solvents show swelling ability from 75% down to 38%, which then correspond to lower actuation efficiencies. There is an overall trend in the swelling ability and the actuation observed. This makes sense since less solvent is taken up, there is less ability to release it. For example, trifluorotoluene (TFT) has much smaller volume and actuation efficiency (75.7%, 5.5%) compared to toluene with similar size and rigidity (92.6%, 18.3%). Another case is 1,1,2-trichlorotrifluoroethane (CFC-113), with size smaller than aromatic solvents, it has only 51.2% of swell volume. (Note: Actuation efficiency was not measured since the gel floats in this solvent). Post synthesis modification to the remaining Si−H bonds, by attaching polarity altering groups could aid in fine
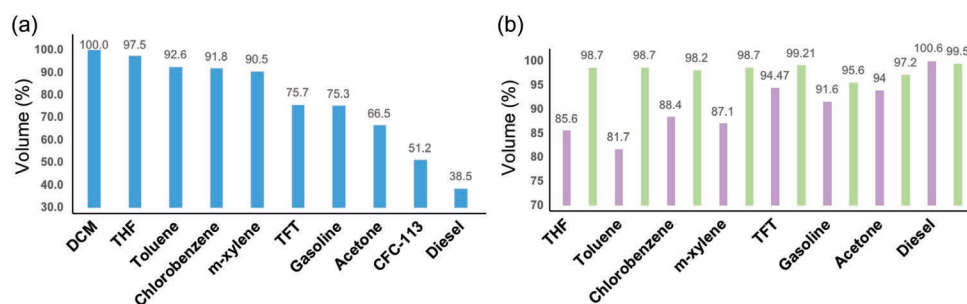

Figure 6. a) Volume of 1:2 (POSS:Azo) gel swollen in different solvents. b) Actuation of the gel under 365 nm UV (purple) and 560 nm vis (green) light normalized versus DCM maximum swell%.
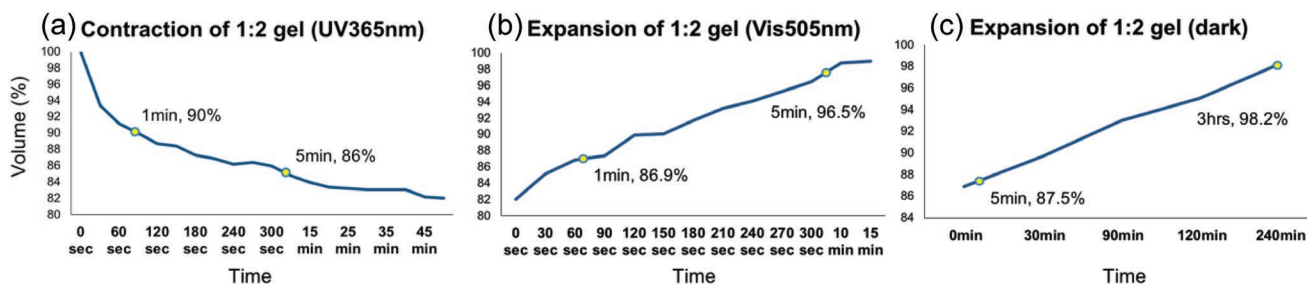
Figure 7. Kinetics of volume change for 1:2 (POSS:Azo) ratio gel in toluene under a) 365 nm UV light, b) 560 nm green light, and c) dark ambient (thermal relaxation).

tuning substance compatibilization. For the rest of the aliphatic chain solvents, longer chain and lower polarity lead to smaller volumes. For example, gasoline (C5–C8) gets to 75.3% of the original volume, while diesel only gets to 38.5% (C10–C14) of initial volume. In diesel, the compactivity of the gel is close to solid state (23.5%), with irradiation of UV light causing a very slight expansion in volume.

2.5. Actuation Efficiency and Photoresponsive Mechanical Properties

To gain insight into the speed of actuation, the time dependence of contraction and expansion were recorded under an optical microscope. The gel with 1:2 (POSS:Azo) ratio was irradiated with 14 mW cm^{-2} of 365 nm UV for 50 min and then 1.7 mW cm^{-2} of 560 nm vis for 30 min (**Figure 7**) in toluene. Toluene was chosen for further investigations since no better solvent system in terms of compatibility was found from the investigation above. The gel reaches 10% of contraction after the first minute and a majority of the volume change (14%) happens within the first 5 min, while an additional 45 min only results in minor changes (2%). Volume change in relaxation is more gradual, but the whole process takes only 10 min to finish. This is expected due to the low intensity of vis light. The gel shows 4.9% of volume increase within the first minute and 13.5% of expansion within 5 min. Generally, the gel reacts to both wavelengths of light relatively quickly and 14% of contraction and expansion can be performed in 10 min. The expansion experiment was repeated in a dark room to determine thermal relaxation without the assistance of light. Only 1.5% of volume

recovery were found in the first 5 min and the gel takes more than 4 h to expand back to its original size.

DMA was conducted on the 1:2 (POSS:Azo) ratio model system in swollen and dry gel forms to test the basic mechanical properties of our materials. The film is also compared. The ability of the gel materials measurement by DMA was surprising, and stems from its relatively high modulus. The swollen gel was measured within a toluene bath to avoid solvent evaporation from within the material at 10 mW cm^{-2} of UV 365 nm light and 2 mW cm^{-2} of vis 560 nm. The storage modulus (G′) of swollen gels switches between 160 and 500 kPa (**Figure 8**a) at 2 mm thickness. The differences between storage moduli are caused by isomerization of azobenzene, which shortens the molecular length and decreases the space between POSS units. The material becomes slightly stiffer with UV light and softens back with vis irradiation. Since the gel is swollen there is significant damping in the material and loss modulus (G″) is incredibly noisy. However, DMA testing of dry gels (0.74 g cm^{-2}) show an opposite effect. In this case, irradiation with UV light causes minor flexibility gain for the dry gel. Storage modulus switches between 460 000 and 510 000 kPa (1.15 mm thick), with loss modulus showing weak but opposite trends. This type of plasticization has been described as a photo-softening effect.[74] In the solid-state, since the structure is compact and locked, isomerization is not capable of lowering the distance between POSS units. Irradiation by UV light helps in organizing the orientation of azobenzenes in the structure, making the gel slightly more flexible. Dry thin film measurements show similar trends to the dry gel, but with much better efficiency (Figure 8b). The storage modulus of the film switches between 190 000 and 300 000 kPa (0.03 mm thick), which has
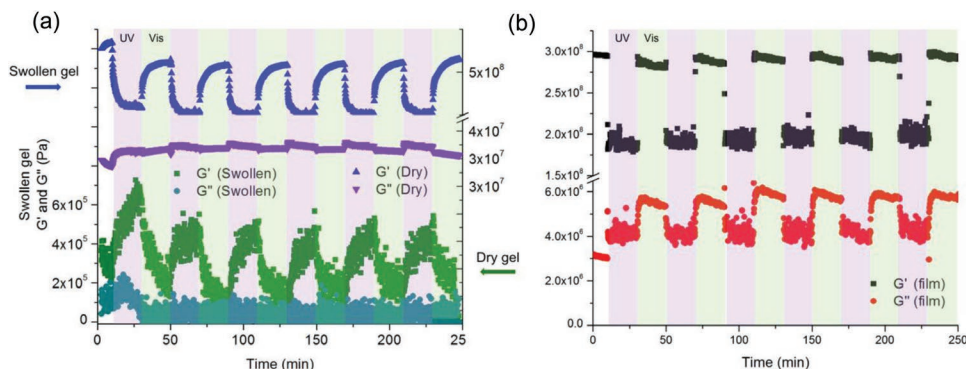

Figure 8. DMA actuation measurements (storage and loss modulus), a) swollen gel/dry gel and b) thin film with 1:2 (POSS:Azo) ratio.
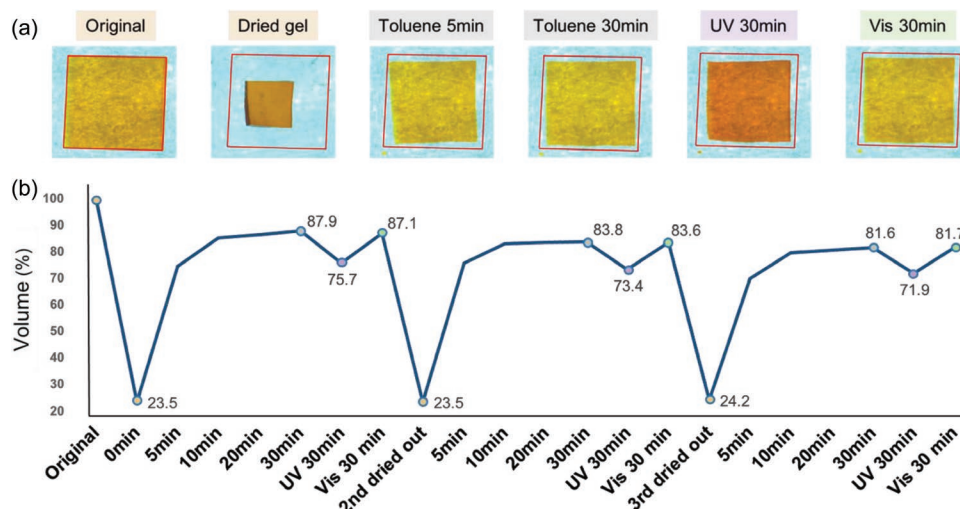
Figure 9. a) Illustration of different states in drying and swelling cycles. b) Volume change process of drying, swelling, and actuating of 1:2 (POSS:Azo) gel over three cycles.

a similar variation ratio as results from the swollen gel. The loss modulus shows similar, but more pronounced trends to that given for the dry gel, with the increase in storage modulus showing a decrease in the imaginary loss component. The differences of thickness are likely the major reason for high light-response efficiency of the film compared to the dried gel. Since both gels and films show moderate modulus change with irradiations, it is promising that with some modifications these materials can be used in practical applications, especially as photodynamic sponges.

2.6. Photodynamic Sponge Behavior of Gels

The goal of our development of these materials was to use them as photodynamic sponges. From the studies above we showed that the 1:2 (POSS:Azo) system performed well in photoresponsive behaviors, but to confirm the similarity between our material and an actual sponge, further experimentation was needed for cyclability and recovery from dried out systems. The gel was air dried to 23.5% of the original volume, and then swollen with toluene again (**Figure 9**a). After sitting in solvent for 30 min, the gel recovered to 87.9% of original size. The first drying/swelling cycle decreases the overall uptake volume due to pore collapse and subsequent inaccessibility. Still the gel can undergo 12.9% contraction and expansion when the size before irradiation is calibrated to 100% (Figure 9b). The second and third cycles show 12.4% and 11.9% of actuation respectfully. Since the surface of the gel dries faster than the interior, uneven shrinking causes deformation, and the tension developed within the structure breaks bonds, decreasing swelling ability. Although the size of the gel decreases slightly with every drying cycle, the gel retains actuation capability. This result shows that our POSS/Azo hybrid system behaves as a working photodynamic sponge, which can endure storage/release and dry/swollen cycles.

Now that the gel has shown potential for photodynamic storage of solvent molecules, a method to better visualize the

process of the gel squeezing or absorbing solvent was proposed. A gel was first swollen in 1 M fluorenone in toluene overnight. The fluorescence from the solution can help with observation when liquid gets squeezed out. The swollen gel was then covered with a layer of water (an incompatible solvent) to minimalize the evaporation of toluene and to limit premature leaching of the dye and toluene (Figure S4, Supporting Information). Actuation of our photodynamic sponge can be easily observed with this design (see Video S2, Supporting Information). At the beginning of irradiation, most UV light is absorbed by azobenzene; hence the gel shows no fluorescence. After a couple seconds, fluorenone solution is squeezed out of the gel, receives UV-light then emits green fluorescence (**Figure 10**). Once the light was switched to vis, we observed the gel gradually expanding and reabsorbing the fluorenone solution. The
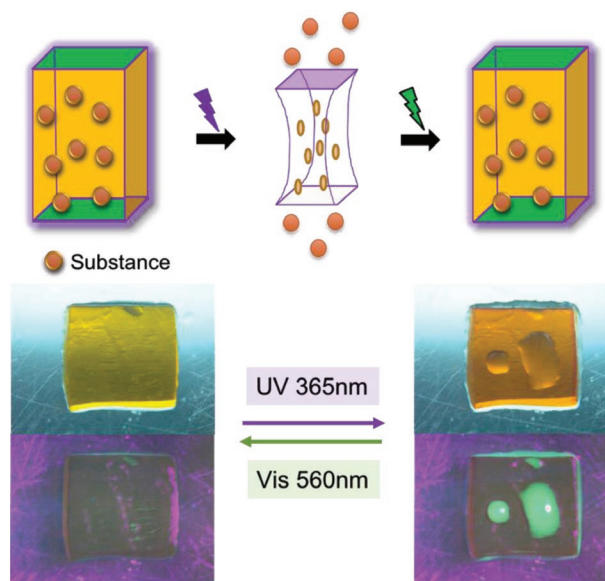

Figure 10. Reversible uptake and release actuation of 1:2 (POSS:Azo) ratio gel under a water bath swollen with 1 M fluorenone solution in toluene.

fluorescent area then shrinks and eventually disappears into the material where it is again quenched by the azobenzene moiety.[75] Furthermore, the removal of gasoline with a dry gel from water has been demonstrated (Figure S9, Supporting Information) as a proof of concept. These results show that storage and release of molecules, especially hydrocarbons in water, can be easily controlled by irradiation wavelength and shows the potential for this system in environmental remediation and soft robotics systems.

3. Conclusions

We have successfully developed an efficient POSS/Azo hybrid network polymer based on a high photoactuation quantum yield azobenzene cross-linker that performs macroscopic photo-driven actuation. A 1:2 (POSS:Azo) ratio was found to offer the best reversible solvent uptake and release performance. Films of the material are able to continuously flip when irradiated on a solvent bed, and up to 18.3% reversible volume reduction is observed by UV irradiation of swollen gels in toluene. Additionally, both systems show reversible modulus and photophysical changes upon cycling irradiation wavelengths up to 10 times. The gel systems behave well as photodynamic sponges over at least three repeat cycles and can soak up hydrophobic solvents such as toluene in a water environment, opening up the door to for use in siloxane based soft robotics and environmental remediation materials for emerging contaminants. The reasoning for the overall ability of this system to expand and contract readily in specific solvents likely stems from a complex combination of structure, elasticity, and swellability. The mechanism is therefore from an amalgamation of molecular length changes, internal polarity, and intrinsic phase changes from altering structural order upon irradiation. Furthermore, excess corner Si—H groups on the POSS materials remain in the structure, offering the additional opportunity for post-synthetic modifications, which enable adjusting the internal polarity of the structure for tuning substance uptake abilities.

4. Experimental Section

Materials: Octakis(dimethylsiloxy)silsesquioxane ($Q_8M_8^H$) was a gift from Mayaterials, inc. Platinum-divinyltetramethyldisiloxane (SIP6831) was obtained from Gelest. Sodium nitrite ($NaNO_2$), phenol, 1,1,2-Trichlorotrifluoroethane (CFC-113), and TFT were obtained from Sigma Aldrich. 4-aminophenol was purchased from Acros Organics. Sodium hydride 60% (NaH) in oil was purchased from TCI America. Allyl bromide, THF, DCM, and toluene were purchased from Alfa Aesar. Hydrochloric acid (HCl), sodium hydroxide (NaOH), and chlorobenzene were purchased from Fisher Scientific. Sulfamic acid was purchased from MC&B Manufacturing Chemists. Diesel fuel and gasoline were purchased from a local gas station. All other solvents were purchased from Millipore-Sigma. All chemicals were used as received.

Syntheses of 4,4'-Dihydroxyazobenzene: 4,4'-dihydroxyazobenzene was prepared by method of Guo et al. with modifications.[76] In a 25 mL round bottom flask, 2 g (18.3 mmol) of 4-aminophenol was mixed with 8.4 mL of HCl (4 mL of 38% HCl were diluted to 8.4 mL) for 1 h. The mixture was cooled to 0 °C in an ice bath. After 20 min, 10 mL of 2 M $NaNO_2$ (1.4 g $NaNO_2$ in 10 mL H_2O) was added dropwise, resulting in the mixture forming a dark red solution. The temperature of the reaction was kept at 0 °C for 2 h then raised with ice bath to room temperature

for 8 h. The resulting solution was light orange in color. Sulfamic acid was added into the mixture to quench excess $NaNO_2$. In a separate 50 mL round bottom flask, 1.72 g (18.3 mmol) of phenol were added into a 2 M NaOH solution (1.47 g of NaOH in 17 mL H_2O) as flask B. The solution in flask A was slowly added into flask B then reacted at room temperature for 12 h. Sulfamic acid was added into the reaction until precipitation occurred. The mixture was left to sit for 5 min then poured into a filter funnel to obtain crude product. The crude product was reprecipitated by ethanol and H_2O, yielding a dark red product (2.763 g, 70.1% yield). ^1H NMR (300 MHz, DMSO-d6, δ): 6.90–6.93 (d, 4H, arH), 7.71–7.73 (d, 4H, arH), 10.14 (s, 2H, Ar—OH). ^{13}C NMR (75.44 MHz, DMSO-d6, δ): 116.25, 124.62, 145.72, and 160.45. LCMS (ESI) m/z: $[M + H]^+$ calculated for C12H10N2O2, 215.07; found 215.15.

Syntheses of 4,4'-Di-allyloxyazobenzene: In a 150 mL round bottom flask, 1 g (4.66 mmol) of 4,4'-dihydroxyazobenzene was dissolved in 70 mL of THF. The solution was then cooled to 0 °C in ice bath. 0.56 g (14 mmol) of NaH was added into the solution. The mixture was then removed from the ice bath and placed in a 70 °C oil bath for 1 h. The mixture was then cooled to 0 °C in an ice bath again, and 1.21 mL (14 mmol) of allyl bromide was added dropwise to the reaction mixture. After the mixture was refluxed for 18 h, solvent was removed by rotary evaporation. The orange product was extracted by DCM. Bright yellow product (0.91 g, yield of 61%) was obtained after recrystallization in THF/methanol. ^1H NMR (300 MHz, CDCl3, δ): 4.63–4.64 (d, 4H, ArOCH2), 5.33–5.50 (m, 4H, CH2=CH), 6.04–6.17 (m, 2H, ArCH2=CH), 7.02–7.05 (d, 4H, ArH), 7.88–7.91 (d, 4H, ArH). ^{13}C NMR (75.44 MHz, CDCl3, δ): 69.02, 114.93, 118.04, 124.34, 132.85, 147.15, and 160.58. LCMS (ESI) m/z: $[M + H]^+$ calculated for C18H18N2O2, 294.14; found 295.35.

Preparation of Azo-POSS polymer film (1:2 POSS/Azo Ratio): A 25 mm × 75 mm glass slide coated with release agent (Pol-Ease 2300) was prepared before the experiment. $Q_8M_8^H$, 0.048 g (0.05 mmol) and 0.033 g (0.1 mmol) of Allyl-Azo was dissolved by 2 mL of toluene in a 20 mL vial with gentle heat (80 °C). After the solution cooled back to room temperature, 7 mg of Karstedt's Catalyst (0.0007 mmol Pt) was mixed with 1 mL of toluene and then added into the mixture of $Q_8M_8^H$ and Allyl-Azo. The mixture was then immediately applied to the glass slide. The slide was covered by a glass dish and allowed to react overnight. After all the solvent had evaporated, the slide with films was placed in a 105 °C oven for 10 min to complete the reaction and remove excess solvent. A freestanding film was then easily removed for further testing. See Supporting Information and text for characterization data.

Preparation of Azo-POSS Polymer Gel (1:2 POSS/Azo Ratio): $Q_8M_8^H$, 0.192 g (0.2 mmol) and 0.13 g (0.4 mmol) of Allyl-Azo was dissolved in 3 mL of DCM in a 20 mL vial with gentle heating. After the solution cooled back to room temperature, 7 mg (0.0007 mmol Pt) of Karstedt's Catalyst-SIP6831 was mixed with 1 mL DCM and then added into the mixture of $Q_8M_8^H$ with Allyl-Azo. In order to prevent the surface of the gel from drying out, 0.25 mL of DCM was added into the vial after 1 h (gelation was already complete). The reaction mixture was then kept in a sealed vial overnight to allow the reaction to go to completion. Samples containing hydride terminated PDMS (450 or 4500 Da were swapped in for $Q_8M_8^H$ using direct molar ratios of hydride groups to maintain approximately the same number of reactive hydride sites. The solvent in the vial was then decanted off, replaced by 10 mL of toluene and allowed to soak for 2 h. This process was repeated three times, after which the polymer was allowed to soak overnight to ensure complete displacement of DCM. The toluene swollen polymer could then be used for testing. The same solvent exchange process was used for the other solvent systems shown in Figure 6. See Supporting Information and text for characterization data.

Electrospray Ionization: Mass of monomers were measured by an LCMS-2010A (Shimadzu, Beachwood, OH, USA). The instrument was set to positive mode with 0.8 L min^{-1} gas flow, 0.08 mL min^{-1} methanol solvent flow and 240 CDL temperature. Detector voltage was set to 1.5 kV. 1 mg of the sample were dissolved in 1 mL of THF and then injected for analysis.

Thermogravimetric Analysis: Degradation of the materials were measured by a TGA-50 (TA Instruments, Inc., New Castle, DE, USA)

instrument. Samples were dried under vacuum and ground before measurement. 10–20 mg of the material was placed in an alumina pan and then heated from room temperature to 900 °C (10 °C min^{-1}) with air flow (60 mL min^{-1}, air), and the ceramic yield and degradation temperature (D5%) recorded.

Rheological Characterization: The rheological properties of gels were collected by a HR2-Discovery hybrid rheometer (TA Instruments, Inc., New Castle, DE, USA). Swollen networks were cut into a cylinder with 8 mm diameter and were then placed between two plates. 0.1 N of axial force, 0.2667% of strain were applied with 10 rd s^{-1} of angular frequency for 90 s. Solvent was continuously applied to ensure full swelling was maintained.

Dynamic Mechanical Analysis: Mechanical properties of solid gel polymers were collected by a DMA8000 (PerkinElmer, Inc., Hopkinton, MA, USA). Network polymer with 1:2 ($Q_8M_8^H$:di-allyloxyazobenzene) molar ratio was cut to 24.5 × 7.0× rectangles with 2.2 mm thickness and then clamped in single cantilever geometry. The instrument analysis head with sample was placed in a toluene bath at room temperature throughout the experiment to ensure the gel stays swollen. Experiments were conducted with 2 N of static force and 0.1 mm of strain. After 10 min of measurement, 20 mW cm^{-2} of UV 365 nm light and 3 mW cm^{-2} of vis 560 nm light were applied on the gel for 20 min each, over 6 cycles. Dried gels with the same composition as swollen gels were cut to 26 mm × 4 mm × 1.15 mm and clamped in the same geometry. Experiments were conducted with 0.25 N of dynamic force and 0.1 mm of strain. Since dried network was more brittle, the force used for measurement was lower than swollen system. After 10 min of measurement, 10 mW cm^{-2} of UV 365 nm light and 2 mW cm^{-2} of vis 560 nm light were applied on the network for 20 min each, for 6 cycles. Films with 0.03 mm thickness were cut to 23 mm × 7 mm and clamped in tension mode due to their more flexible structure. Experiments were conducted with auto-tension drive with 0.1 mm of strain. After 10 min of measurement, 30 mW cm^{-2} of UV 365 nm light and 6.5 mW cm^{-2} of vis 560 nm light were applied on the film for 20 min each, for 6 cycles.

Specific Surface Area and Porosity Analyses: A Micromeritics 3FLEX surface and catalyst characterization analyzer (Micromeritics Inc., Norcross, GA) was used to analyze surface area and porosity of all samples. Samples were ground and then placed in high vacuum for 4 h for degassing. The samples then were moved to sample tubes, and flushed with nitrogen gas for 30 min to ensure the absence of unwanted gases. Starting from 0.8 (P/P_0) relative pressure, measurements were conducted with 12 data points increasing at 0.05 (P/P_0) relative pressure at −196 °C (77 K). The surface area and pore size distribution were calculated by BET and Density Functional Theory methods, respectively.

Optical Microscopy: Microscope images were taken by a STEMI 2000-C (ZEISS, White plains, NY, USA). The gels with different $Q_8M_8^H$/di-allyloxyazobenzene ratios were cut to 4.5 × 4.5 squares with 1.25 mm thickness, then soaked in toluene in a Petri dish of 50 mm diameter. UV 365 nm and vis 505 nm LED lamps were applied from the side at ≈30° angle with 14 and 1.7 mW cm^{-2} intensities, respectively. The gel was adjusted to the middle of observing window and an image was taken from the microscope. After UV irradiation for 30 min, another image was taken without moving the gel. The gel then was irradiated with vis light for 30 min then another image was taken. The volume of the gel in three stages were measured from the images then compared.

NMR Spectroscopy: NMR spectra were collected from an AVANCE III spectrometer (Bruker) at 300 MHz. 4,4′-dihydroxyazobenzene was dissolved in DMSO-d6 and allyl-azo in chloroform-d for measurements. ^{1}H NMR spectra were collected with 16 scans and 20 ppm window width. ^{13}C NMR were collected with 4096 scans and 240 ppm window width.

UV–vis Spectroscopy: Spectra were collected from Shimadzu UV-2600 (Shimadzu, Beachwood, OH, USA). allyl-azo were dissolved in toluene and scanned from 900 to 200 nm with 1 nm resolution. Quantum yield of isomerization for three solutions in toluene (M = 0.00003494, 0.00004581, 0.00006522 mole L^{-1}) was calculated with program developed by Stranius and Börjesson with trans azobenzene as the photostationary position.[69] Quantum yield of cis-trans back relaxation under 365 nm irradiation was ignored. Molar absorptivities of trans and cis form of allyloxyazobenzene were calculated from $\pi–\pi*$ transition peaks at 358 and 309 nm, respectively.

Fourier-Transform Infrared Spectroscopy: Spectra were measured by Thermo Scientific Nicolet iS5 (Waltham, Massachusetts, MA, USA). Attenuated total reflection method was applied. Samples were measured from 4000 to 400 cm^{-1} with 0.121 cm^{-1} spacing on a ZnSe crystal.

Scanning Electron Microscopy: Images were taken on a Hitachi S2700 (Hitachi High-Tech America, Schaumburg, IL, USA) with lanthanum hexaboride as source. Dried gels were placed on a sample holder then sputter coated with Au/Pd. Images were collected with 70, 200, and 2000× magnification with 20 kV voltage.

Supporting Information

Supporting Information is available from the Wiley Online Library or from the author.

Conflict of Interest

The authors declare no conflict of interest.

Data Availability Statement

Research data are not shared.

[1] P. J. Roth, A. B. Lowe, *Polym. Chem.* **2017**, *8*, 10.

[2] U. Jeong, Y. Yin, *Adv. Funct. Mater.* **2020**, *30*, 1907059.

[3] M. Karimi, A. Ghasemi, P. Sahandi Zangabad, R. Rahighi, S. M. Moosavi Basri, H. Mirshekari, M. Amiri, Z. Shafaei Pishabad, A. Aslani, M. Bozorgomid, D. Ghosh, A. Beyzavi, A. Vaseghi, A. R. Aref, L. Haghani, S. Bahrami, M. R. Hamblin, *Chem. Soc. Rev.* **2016**, *45*, 1457.

[4] Y. Jiang, H. Wang, S. Li, W. Wen, *Sensors* **2014**, *14*, 6952.

[5] T. Chen, R. Ferris, J. Zhang, R. Ducker, S. Zauscher, *Prog. Polym. Sci.* **2010**, *35*, 94.

[6] B. H. Shen, G. M. Veith, W. E. Tenhaeff, *Sci. Rep.* **2018**, *8*, 11549.

[7] A. Lendlein, S. Kelch, *Angew. Chem. Int. Ed. Engl.* **2002**, *41*, 2034.

[8] L. Sun, W. M. Huang, Z. Ding, Y. Zhao, C. C. Wang, H. Purnawali, C. Tang, *Mater. Des.* **2012**, *33*, 577.

[9] P. Xiao, J. Zhang, J. Zhao, M. H. Stenzel, *Prog. Polym. Sci.* **2017**, *74*, 1.

**ADVANCED
SCIENCE NEWS**

www.advancedsciencenews.com

**ADVANCED
FUNCTIONAL
MATERIALS**

www.afm-journal.de

[10] A. H. Gelebart, D. Liu, D. J. Mulder, K. H. J. Leunissen, J. van Gerven, A. P. H. J. Schenning, D. J. Broer, *Adv. Funct. Mater.* **2018**, *28*, 1705942.

[11] H. J. Cho, M. Chung, M. S. Shim, *J. Ind. Eng. Chem.* **2015**, *31*, 15.

[12] L. Florea, A. Hennart, D. Diamond, F. Benito-Lopez, *Sens. Actuators, B* **2012**, *175*, 92.

[13] J. Zhang, J. Wang, H. Tian, *Mater. Horiz.* **2014**, *1*, 169.

[14] J. Scheerder, D. J. Walton, I. R. Peterson, L. S. Miller, *Adv. Mater. Opt. Electron.* **1998**, *8*, 309.

[15] F. Ercole, T. P. Davis, R. A. Evans, *Polym. Chem.* **2010**, *1*, 37.

[16] O. Bertrand, J. F. Gohy, *Polym. Chem.* **2017**, *8*, 52.

[17] L. Florea, D. Diamond, F. Benito-Lopez, *Macromol. Mater. Eng.* **2012**, *297*, 1148.

[18] Y. Wu, Y. Wei, Y. Ji, *Polym. Chem.* **2020**, *11*, 5297.

[19] Y. Zakrevskyy, M. Richter, S. Zakrevska, N. Lomadze, R. Von Klitzing, S. Santer, *Adv. Funct. Mater.* **2012**, *22*, 5000.

[20] N. Katsonis, M. Lubomska, M. M. Pollard, B. L. Feringa, P. Rudolf, *Prog. Surf. Sci.* **2007**, *82*, 407.

[21] M. Irie, T. Fukaminato, K. Matsuda, S. Kobatake, *Chem. Rev.* **2014**, *114*, 12174.

[22] R. Klajn, *Chem. Soc. Rev.* **2014**, *43*, 148.

[23] C. R. Crecca, A. E. Roitberg, *J. Phys. Chem. A* **2006**, *110*, 8188.

[24] T. Fujino, S. Y. Arzhantsev, T. Tahara, *Bull. Chem. Soc. Jpn.* **2002**, *75*, 1031.

[25] H. M. D. Bandara, S. C. Burdette, *Chem. Soc. Rev.* **2012**, *41*, 1809.

[26] E. Merino, *Chem. Soc. Rev.* **2011**, *40*, 3835.

[27] S. L. Oscurato, M. Salvatore, P. Maddalena, A. Ambrosio, *Nanophotonics* **2018**, *7*, 1387.

[28] F. P. Nicoletta, D. Cupelli, P. Formoso, G. de Filpo, V. Colella, A. Gugliuzza, *Membranes* **2012**, *2*, 134.

[29] Z. Mahimwalla, K. G. Yager, J. I. Mamiya, A. Shishido, A. Priimagi, C. J. Barrett, *Polym. Bull.* **2012**, *69*, 967.

[30] A. Goulet-Hanssens, F. Eisenreich, S. Hecht, *Adv. Mater.* **2020**, *32*, 1905966.

[31] S. T. Zheng, H. H. Yin, Z. G. Ma, N. L. Sheng, T. G. Zhan, X. Y. Yan, J. Cui, L. J. Liu, K. D. Zhang, *Chinese Chem. Lett.* **2019**, *30*, 707.

[32] M. Dong, A. Babalhavaeji, S. Samanta, A. A. Beharry, G. A. Woolley, *Acc. Chem. Res.* **2015**, *48*, 2662.

[33] I. N. Lee, O. Dobre, D. Richards, C. Ballestrem, J. M. Curran, J. A. Hunt, S. M. Richardson, J. Swift, L. S. Wong, *ACS Appl. Mater. Interfaces* **2018**, *10*, 7765.

[34] Y. J. Choi, J. T. Kim, W. J. Yoon, D. G. Kang, M. Park, D. Y. Kim, M. H. Lee, S. K. Ahn, K. U. Jeong, *ACS Macro Lett.* **2018**, *7*, 576.

[35] A. Liu, C. Xiong, X. Ma, W. Ma, R. Sun, *Chinese J. Chem.* **2019**, *37*, 793.

[36] D. Corbett, M. Warner, *Liq. Cryst.* **2009**, *36*, 1263.

[37] D. Iqbal, M. H. Samiullah, *Materials* **2013**, *6*, 116.

[38] M. Pilz Da Cunha, E. A. J. Van Thoor, M. G. Debije, D. J. Broer, A. P. H. J. Schenning, *J. Mater. Chem. C* **2019**, *7*, 13502.

[39] J. A. Lv, W. Wang, W. Wu, Y. Yu, *J. Mater. Chem. C* **2015**, *3*, 6621.

[40] Y. Zhang, Y. Ma, J. Sun, *Langmuir* **2013**, *29*, 14919.

[41] C. Qin, Y. Feng, H. An, J. Han, C. Cao, W. Feng, *ACS Appl. Mater. Interfaces* **2017**, *9*, 4066.

[42] F. Zhang, J. Fan, P. Zhang, M. Liu, J. Meng, L. Jiang, S. Wang, *N. P. G. Asia Mater.* **2017**, *9*, e380.

[43] S. K. Ahn, T. H. Ware, K. M. Lee, V. P. Tondiglia, T. J. White, *Adv. Funct. Mater.* **2016**, *26*, 5819.

[44] D. Y. Kim, S. Shin, W. J. Yoon, Y. J. Choi, J. K. Hwang, J. S. Kim, C. R. Lee, T. L. Choi, K. U. Jeong, *Adv. Funct. Mater.* **2017**, *27*, 1606294.

[45] N. Begum, S. Kaur, Y. Xiang, H. Yin, G. Mohiuddin, N. V. S. Rao, S. K. Pal, *J. Phys. Chem. C* **2019**, *24*, 874.

[46] E. Besson, A. Mehdi, D. A. Lerner, C. Reyé, R. J. P. Corriu, *J. Mater. Chem.* **2005**, *15*, 803.

[47] T. J. White, D. J. Broer, *Nat. Mater.* **2015**, *14*, 1087.

[48] T. J. White, *J. Polym. Sci., Part B: Polym. Phys.* **2018**, *56*, 695.

[49] D. Wang, J. Song, S. Lin, J. Wen, C. Ma, Y. Yuan, M. Lei, X. Wang, N. Wang, H. Wu, *Adv. Funct. Mater.* **2019**, *29*, 1901009.

[50] Y. Liu, X. Wang, S. Feng, *Adv. Funct. Mater.* **2019**, *29*, 1902488.

[51] Y. L. Zhao, J. F. Stoddart, *Langmuir* **2009**, *25*, 8442.

[52] A. M. Rosales, C. B. Rodell, M. H. Chen, M. G. Morrow, K. S. Anseth, J. A. Burdick, *Bioconjugate Chem.* **2018**, *29*, 905.

[53] K. Peng, I. Tomatsu, A. Kros, *Chem. Commun.* **2010**, *46*, 4094.

[54] Y. Takashima, S. Hatanaka, M. Otsubo, M. Nakahata, T. Kakuta, A. Hashidzume, H. Yamaguchi, A. Harada, *Nat. Commun.* **2012**, *3*, 1270.

[55] L. Ionov, *Mater. Today* **2014**, *17*, 494.

[56] Y. Lin, H. R. Hansen, W. J. Brittain, S. L. Craig, *J. Phys. Chem. B* **2019**, *123*, 8492.

[57] R. H. Zha, G. Vantomme, J. A. Berrocal, R. Gosens, B. De Waal, S. Meskers, E. W. Meijer, *Adv. Funct. Mater.* **2018**, *28*, 1703952.

[58] S. Guo, A. Sugawara-Narutaki, T. Okubo, A. Shimojima, *J. Mater. Chem. C* **2013**, *1*, 6989.

[59] J. Garcia-Amors, D. Velasco, *Advanced Elastomers – Technology, Properties and Applications*, IntechOpen, London **2012**.

[60] S. Guo, K. Matsukawa, T. Miyata, T. Okubo, K. Kuroda, A. Shimojima, *J. Am. Chem. Soc.* **2015**, *137*, 15434.

[61] S. Guo, T. Okubo, K. Kuroda, A. Shimojima, *J. Sol-Gel Sci. Technol.* **2016**, *79*, 262.

[62] H. Finkelmann, H. J. Kock, G. Rehage, D. M. Chemie, *Rapid Commun* **1981**, *2*, 317.

[63] M. Abboud, A. Sayari, *Microporous Mesoporous Mater.* **2017**, *249*, 157.

[64] D. Pan, E. Yi, P. H. Doan, J. C. Furgal, M. Schwartz, S. Clark, T. GoodsonIii, R. M. Laine, *J. Ceram. Soc. Japan* **2015**, *123*, 756.

[65] J. V. Accardo, J. A. Kalow, *Chem. Sci.* **2018**, *9*, 5987.

[66] J. C. Furgal, C. U. Lenora, *Phys. Sci. Rev.* **2019**, *5*, 1.

[67] R. M. Laine, *J. Mater. Chem.* **2005**, *15*, 3725.

[68] N. H. Hu, C. U. Lenora, T. A. May, N. C. Hershberger, J. C. Furgal, *Mater. Chem. Front.* **2020**, *4*, 851.

[69] K. Stranius, K. Börjesson, *Sci. Rep.* **2017**, *7*, 41145.

[70] M. Chen, B. Yao, M. Kappl, S. Liu, J. Yuan, R. Berger, F. Zhang, H. J. Butt, Y. Liu, S. Wu, *Adv. Funct. Mater.* **2020**, *30*, 1906752.

[71] D. Pan, E. Yi, P. H. Doan, J. C. Furgal, M. Schwartz, S. Clark, T. Goodson, R. M. Laine, *J. Ceram. Soc. Japan* **2015**, *123*, 756.

[72] Y. Liu, W. Yang, H. Liu, *Chem. - Eur. J.* **2015**, *21*, 4731.

[73] L. Sun, R. F. Gibson, F. Gordaninejad, J. Suhr, *Compos. Sci. Technol.* **2009**, *69*, 2392.

[74] J. M. Harrison, D. Goldbaum, T. C. Corkery, C. J. Barrett, R. R. Chromik, *J. Mater. Chem. C* **2015**, *3*, 995.

[75] S. Saeed, P. A. Channar, A. Saeed, F. A. Larik, *J. Photochem. Photobiol. A Chem.* **2019**, *369*, 159.

[76] S. Guo, W. Chaikittisilp, T. Okubo, A. Shimojima, *RSC Adv.* **2014**, *4*, 25319.